



# Earth and Space Science

## TECHNICAL REPORTS: DATA

10.1029/2019EA000876

**Key Points:**

- We obtain a new data set of rheology measurements from naturally occurring hemipelagic sediment and a terrestrial mud volcano
- Comparison with existing measurements indicates that particle composition influences yield stress and consistency
- Most pumice clasts recovered from IODP 340 are stratigraphically in place and thus date the occurrence of eruptions

**Supporting Information:**

- Supporting Information S1
- Table S1

**Correspondence to:**

M. Manga,  
manga@seismo.berkeley.edu

**Citation:**

Knappe, E., Manga, M., Le Friant, A., & the IODP 340 scientists (2020). Rheology of Natural Sediments and Its Influence on the Settling of Dropstones in Hemipelagic Marine Sediment. *Earth and Space Science*, 7, e2019EA000876. <https://doi.org/10.1029/2019EA000876>

Received 4 SEP 2019

Accepted 27 JAN 2020

Accepted article online 3 FEB 2020

## Rheology of Natural Sediments and Its Influence on the Settling of Dropstones in Hemipelagic Marine Sediment

**E. Knappe<sup>1,2</sup> , M. Manga<sup>1</sup> , A. Le Friant<sup>3</sup>, and the IODP 340 scientists**

<sup>1</sup>Department of Earth and Planetary Science, University of California, Berkeley, CA, USA, <sup>2</sup>Geoscience Department, University of Montana, Missoula, MT, USA, <sup>3</sup>Institut de Physique du Globe de Paris, Paris, France

**Abstract** We investigate the rheology of naturally occurring hemipelagic marine sediment and compare measurements to another naturally occurring sediment from a terrestrial mud volcano and literature values. The hemipelagic marine sediment, collected by IODP 340, has a median grain size of 5.5 microns, is poorly sorted, and contains 31% clay, including smectite. The yield stresses and consistency are calculated by applying a range of shear stresses and shear rates using a cone-and-plate rheometer. A Herschel-Bulkley model is fit to measured shear stresses and shear rates to calculate the yield stress and consistency. These measurements are performed at a range of particle concentrations and show that the hemipelagic sediment has a yield stress at particle concentrations as low as 10%. Increasing particle concentration increases the yield stress and consistency. We apply our results to show that natural pumice clasts need to have a radius greater than about 1 cm in order to settle through hemipelagic sediment on the sea floor. Most recovered pumice clasts from IODP 340 are thus preserved in the same horizon in which they were deposited.

### 1. Introduction

The rheological properties of sediment are influenced by multiple factors including particle concentration, size, size distribution, composition, and pore-water salinity (Imran et al., 2001). Models for sediment rheology are often based on laboratory characterization of idealized kaolinite and montmorillonite mixtures (e.g., Marr et al., 2001; Baas & Best, 2002; Talling, 2013). These idealized mixtures differ from naturally occurring submarine sediment in particle size and size distribution as well as composition. There are few studies of the rheology of natural submarine deposits (e.g., Imran et al., 2001; Jeong, 2013; Locat et al., 2004; Menapace et al., 2019).

The composition of the sediment can affect its rheology and cohesive sediments exhibit complex behaviors that are often difficult to characterize (Yang et al., 2014). When materials contain high clay fractions, strong attractive colloidal forces can lead to thixotropic behavior, that is, the viscosity of the material depends on the shear history (Santolo & Evangelista, 2005). Thixotropy is caused by a time-dependent microstructural evolution of a material. When a shear stress or strain is applied to the material the viscosity decreases (Barnes, 1997). In sediment, this decrease in viscosity could be caused by the particles developing a preferred orientation or by the breakdown of flocs and aggregates that release entrapped fluid and increases the lubrication between the particles (Barnes, 1997; Treger et al., 2010). However, this evolution is reversible: The longer a material is at rest, the more the microstructure rebuilds until it reaches its initial state again.

In addition to the clay fraction, the type of clay can also influence rheology due to differences in cohesion. Smectite and montmorillonite have high cohesion compared to kaolinite and illite. The difference in cohesion affects how easily the microstructure can be broken down. Naturally occurring sediments differ from idealized mixtures because they contain a range of sediment sizes, fossils, minerals, and clays.

Thixotropy is also influenced by salinity and particle concentration. At high salinity, greater than 0.35 to 0.55 g/L, the interparticle forces are strong enough to favor fast reconstruction of the microstructure, thus making the material strongly thixotropic (Perret et al., 1996). Particle concentration also affects the thixotropic behavior of a material. At low particle concentrations, there are fewer interactions between the particles and thixotropic effects are less significant (Santolo et al., 2012).

©2020. The Authors.

This is an open access article under the terms of the Creative Commons Attribution License, which permits use, distribution and reproduction in any medium, provided the original work is properly cited.

The rheological behavior of sediment has implications for the initiation and flow of submarine sediment-laden density currents. Additionally, seafloor sediment preserves a record of volcanic eruptions in tephra and crypto-tephra layers including isolated centimeter-sized pumice clasts that record the occurrence of additional volcanic eruptions (Le Friant et al., 2015, 2013; Palmer et al., 2016; Jutzeler et al., 2016). These eruptions can be dated using the surrounding sediments, but this assumes that the clasts are at the same stratigraphic location and did not settle through underlying sediment upon deposition.

In this study we analyze naturally occurring hemipelagic sediment collected from the seafloor adjacent to Lesser Antilles Volcanic Arc. To determine yield stress and consistency as a function of particle concentration a suite of rheometric tests are utilized. The yield stress and consistency of a material depend strongly on the particle concentration. As particle concentration increases, there is an increase in particle-particle interactions, which causes an increase in the friction and thus increases the yield stress and consistency (Coussot & Piau, 1994). We thus use a range of particle concentrations to develop a better understanding of how these natural sediments flow. The same tests are performed on an additional naturally occurring sediment from the Davis-Schrimpf mud volcanoes for further comparison. Additionally, our results are compared to previously published measurements on other materials in order to better identify the factors that influence rheology. For illustrative purposes, we use our results to determine the size of particles that would settle through the hemipelagic sediment on the seafloor and hence what size particles would be preserved in situ within marine sediments. We use these results to assess whether volcanic dropstones collected by IODP 340 are preserved in situ.

## 2. Methods

The hemipelagic sediment was collected offshore of the Lesser Antilles volcanic arc from a water depth of 2,745 m. The Lesser Antilles volcanic arc is located at the eastern border of the Caribbean plate. The proximity of our sampling location to volcanic islands, specifically the active volcano Montagne Pelée, causes our sample to contain volcaniclastic sediment as well as marine fossils (Le Friant et al., 2008). The sample, 340 U1400C 3H 4, was collected during IODP 340 from 26 m below the sea floor from a sedimentary unit that includes multiple landslide deposits (Le Friant et al., 2013; Lafuerza et al., 2014; Brunet et al., 2016); see supporting information Figure S1a for a location map. For comparison, another natural mud from the Davis-Schrimpf mud volcanoes located next to the Salton Sea in the Imperial Valley, California, is analyzed (map in supporting information Figure S1b). The Salton Sea mud volcanoes are driven by the ascent of CO<sub>2</sub> from underlying geothermal systems and the mud recirculates within the subsurface plumbing system (Svensen et al., 2009).

### 2.1. Sample Properties

Size distribution is measured using a Sequoia Portable XR Laser Diffraction Particle Size Analyzer. The cumulative size distribution for both samples is shown in Figure 1a. The median grain size for the hemipelagic sediment is 5.5 microns. Grain density was measured as 2,700 kg/m<sup>3</sup> on the IODP ship using helium pycnometry (Le Friant et al., 2013).

Particle concentration, the amount of solids in the total mixture, is given by

$$\phi = \frac{V_s}{V_t} \quad (1)$$

where  $V_s$  the volume of solids and  $V_t$  is the total volume. We measure  $\phi$  by weighing a known volume of material. Uncertainty in  $\phi$  is dominated by uncertainty in measured volume. The grain density of the hemipelagic sediment was confirmed to be 2,700 kg/m<sup>3</sup>.

Figures 1b and 1c show three-dimensional X-ray microtomography reconstructions of the samples imaged at the Advanced Light Source 8.3.2 beamline, Lawrence Berkeley National Laboratory, with a resolution of 1.3 microns/pixel. The hemipelagic marine sediment is poorly sorted and contains large voids (Figure 1b). Additionally, the sediment also contains foraminifera fossils and crystal fragments, such as hornblende, quartz, and muscovite, that are large compared to particles in the surrounding matrix. The Salton Sea sediment has a more uniform size distribution by comparison (Figure 1c).

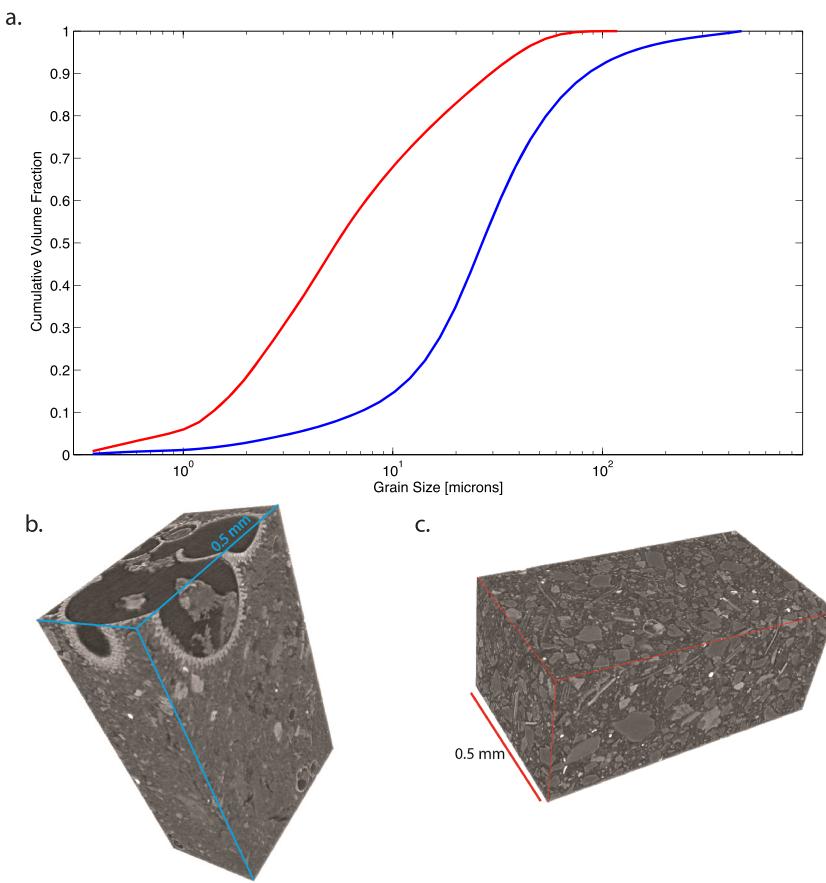


**Figure 1.** (a) The mean cumulative size distribution of the sediments. The hemipelagic sediment, shown in blue, is the average of four tests, and the Salton Sea sediment, shown in red, is the average of two tests. (b) Three-dimensional microtomography reconstructions of the materials. Reconstruction of the hemipelagic sediment, which is poorly sorted and contains large fossils. (c) Reconstruction of the Salton Sea sediment, which is much more uniform in size than the hemipelagic sediment.

Using X-ray diffraction, we determine that the hemipelagic sediment is composed of 20% feldspar and plagioclase, 19% calcite, 16% quartz, 7% aragonite, and 31% clay. The Salton Sea sediment is composed of 41% quartz, 3% dolomite, 16% plagioclase, 8% orthoclase, and 26% clay. The clay in both samples contains kaolinite, illite, and montmorillonite, while the hemipelagic sediment also contains smectite.

### 3. Rheology Measurement Methods

We measure the rheology using a HAAKE Rheoscope 1. To ensure uniform strain rate through the sample a cone-and-plate geometry, with a 4° cone angle and 60-mm-diameter plate, is used. We apply either a controlled angular velocity and hence a shear rate and then measure the torque required to maintain this rate or alternatively apply a torque and measure the resulting deformation.

In order to prevent slippage, both the cone and the plate are covered in ANSI 150 grit sand paper (average particle size of 100 microns). The gap size between the plate and the center of the cone was 0.142 mm after adhesion of sand paper. Each test utilizes 8 ml of sample. To prevent jamming of particles within the gap, the mud is sieved to remove particles larger than 100 microns, which comprise less than a few percent of the volume of the sediment. The volumetrically dominant fine particles have a larger controlling influence on the yield stress, so we do not expect that the small number of fossils removed from the sample would alter the rheology (Yu et al., 2013). In order to prevent temperature fluctuations from affecting the measurements, the temperature of the mud is kept constant at 20 °C using a Thermo Scientific Haake DC30-K20 Digital Bath. At this temperature water viscosity is 1.05 mPa·s compared to 1.57 mPa·s at a seafloor temperature

of 4 °C. The performed tests should accurately estimate the rheologic parameters since the yield stress is dependent on particle interactions and will not vary due to temperature. However, the consistency will be higher at sea bottom temperatures.

The hemipelagic sediment is from a marine setting so we control salinity of the water by adding artificial seawater since the salinity of the water affects suspension rheology (Jeong, 2010). Thirty-five grams of Instant Ocean salt mixture is added to 1 L of water to create salinity similar to that of the Caribbean Sea.

The thixotropic nature of the sediment led us to focus on the static yield stress, above which the material will start to flow, and the dynamic yield stress, below which the material will no longer flow. Two separate tests are performed: the first to quantify the static yield and the second to determine the dynamic yield and consistency.

### 3.1. Flow Characteristics

In order to characterize rheology we consider an idealized constitutive model. The most frequently used model to describe naturally occurring sediments and muds is the Herschel-Bulkley model (Huang & García, 1998):

$$\tau = \tau_y + K\dot{\gamma}^n, \quad (2)$$

where  $\tau$  is shear stress,  $\tau_y$  is the yield stress,  $\dot{\gamma}$  is strain rate,  $K$  is consistency, and  $n$  is the flow index. We adopt the Herschel-Bulkley model, but note that models without a yield stress have also been used to model mud rheology especially for low strain rates and high viscosities (e.g., Menapace et al., 2019).

During the measurements, it became apparent that both materials did not simply follow the Herschel-Bulkley model (supporting information Figure S2) as has been documented previously (e.g., Yang et al., 2014). Different stresses are measured when applying increasing and decreasing strain rates, indicating that the properties are history dependent, one signature of thixotropic rheology (Moller et al., 2009) (supporting information Figure S2b). This leads to the static yield stress, which is associated with the start of flow, being higher than the dynamic yield stress, below which the material will stop flowing, due to the static yield stress having to breakdown the microstructure that has formed while the material was at rest. The microstructure breakdown is reversible; if the material is left at rest, the yield stress will increase again (Moller et al., 2009). There are models that quantify the evolving microstructure (e.g., de Souza Mendes, 2009; Dullaert & Mewis, 2006); however, for this study we focus on the static yield stress and the dynamic yield stress. Consistency is analogous to viscosity and is also quantified prior to the cessation of flow.

### 3.2. Static Yield

Thixotropic fluids have a viscosity that decreases over time as they are sheared. To mitigate the variations in shear history, samples are allowed to rest for 10 min between each test (Van Kessel & Blom, 1998). After running hysteresis tests at varying time intervals between tests, the material recovers most of its strength after 10 min. Ten minutes limits the amount of evaporation of water and settling of particles so as to not affect measurements. Static yield is measured using a controlled stress mode while the sample was maintained at a constant temperature. For this controlled stress mode, an increasing shear stress,  $\tau$ , or torque, is applied and the resulting deformation is measured (supporting information Figure S2a). Shear stress is increased linearly in 70 steps from 0 to 1,500 Pa, for 10 s each step. Initially, strain increases linearly with stress, however with further increases of stress the strain grows exponentially fast and is immeasurable after a certain shear stress. The location of this exponential increase varied with each test depending on the water content. To calculate static yield stress a Herschel-Bulkley model is fit to the data from increasing portion of the test, providing  $\tau_y$ ,  $K$ , and  $n$ .

### 3.3. Dynamic Yield

In order to determine the dynamic yield stress and the consistency, a shear strain rate,  $\dot{\gamma}$ , is applied and the torque, or shear stress,  $\tau$ , required to maintain this strain rate is measured. Strain rate is increased in 40 steps uniformly spaced in the log of strain rate from 0.01 to  $1.5 \text{ s}^{-1}$ , and subsequently decreased in the same 40 steps, with each step lasting 15 s (supporting information Figure S3 shows results for two different particle concentrations). To determine the dynamic yield stress and consistency, the decreasing portion of the test is fit with a Bingham model.

## 4. Results

Figure 2a shows the relationship between particle concentration (%) and yield stress (Pa) for our samples compared to other studies. For the hemipelagic sediment and Salton Sea mud, the filled circles show static yield stress and the open circles show dynamic yield stress. Table 1 summarizes the results for our study, and supporting information Table S1 summarizes comparative studies. In our samples the dynamic yield stress is always lower than the static yield stress, with the exception of the Salton Sea mud at a concentration of 40.5%. This exception could be the result of sedimentation within the sample that allowed the material to start flowing at a lower static yield stress. In addition to measuring the static yield using a controlled stress mode, we can estimate the static yield from the inflection point of the increasing strain rate portion of the dynamic yield tests (Santolo et al., 2012), and the two separately determined yield stresses are similar.

A yield stress becomes apparent in the hemipelagic sediment at a particle concentration of ~10% and increases with increasing particle concentration. Figure 2a also shows the yield stress as a function of particle concentration measured in other studies (Cousset & Piau, 1994; Cousset et al., 1996; Huang & García, 1998; Malet et al., 2005; Remaitre et al., 2005; Maciel et al., 2009; Santolo et al., 2010; Blasio et al., 2011; Manga & Bonini, 2012; Jeong, 2013; Yang et al., 2014; Tran et al., 2015). In Figure 2, non-natural sediments are represented with squares.

To determine the yield stress as a function of particle concentration, the hemipelagic data is fit with the model developed by Mueller et al. (2009):

$$\tau_y = \tau^* \left( \left( 1 - \frac{\phi}{\phi_m} \right)^{-2} - 1 \right), \quad (3)$$

where  $\tau^*$  is a fitting parameter,  $\phi$  is the particle concentration,  $\phi_m$  is the maximum particle concentration. The fit of the Mueller et al. (2009) model to the hemipelagic static yield data is shown in supporting information Figure S4. We find  $\tau^* = 34.9 \pm 6.9$  Pa and  $\phi_m = 0.23 \pm 0.004$ .

Consistency also increases with increasing particle concentration. Following Mader et al. (2013), the hemipelagic data are fit to the model:

$$K_r = \left( 1 - \frac{\phi}{\phi_m} \right)^{-2}, \quad (4)$$

where  $K_r = K/\mu_0$  where  $\mu_0$  is viscosity of the suspending fluid (Pa·s) (supporting information Figure S5). We find  $\phi_m = 0.25 \pm 0.02$  Pa and  $\mu_0 = 0.14 \pm 0.05$  Pa·s.

## 5. Discussion

Both the static and dynamic yield tests indicate that the hemipelagic sediment is thixotropic. In the dynamic tests, there is a significant difference between the increasing strain rate section and the decreasing strain rate section (Supporting Information Figure S2b). This indicates that the material has a history dependence in its rheology and hence its microstructure. The higher the particle concentration, the more dramatic this hysteresis. In the static yield tests, the material initially behaves like a linear elastic material until a specific stress is overcome and then the strain exponentially increases until the material reaches another critical point and flows too fast for the rheometer to measure (Supporting Information Figure S2a). Cousset et al. (1992) similarly found that the response of their clay-rich material is essentially elastic until a critical point is reached and the flow becomes unstable and fast. This behavior indicates that the material is initially structured, but when the apparent yield stress is overcome the sediment becomes unstructured and starts to flow at increasing velocities. Alignment of particles with the flow causes the material to flow faster when a shear is applied (Barnes, 1997). Additionally, the static yield stress is significantly larger than the dynamic yield stress, which is consistent with thixotropic behavior (Figure 2).

The scatter within our data could be caused by the history dependence of our samples due to slightly different handling of the material prior to testing. We tried to mitigate this effect by allowing the samples to rest between tests and by loading the samples into the rheometer in the same way. The scatter could additionally

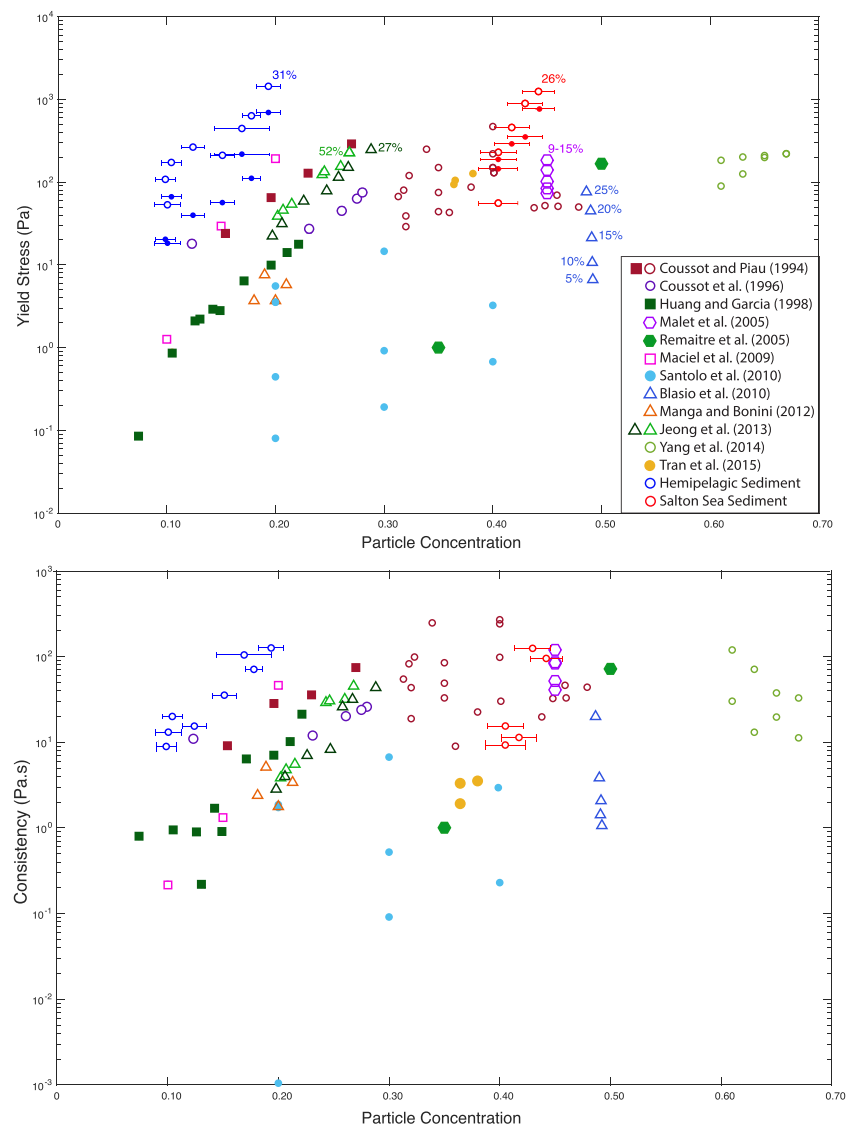


**Figure 2.** (a) Yield stress as a function of particle concentration from multiple different studies and (b) consistency as a function of particle concentration from multiple different studies. Clay contents shown in numbers next to the respective data when reported. For our measurements, open symbols show static yield stress and filled symbols show dynamic yield stress. All data in Table 1 and supporting information Table S1.

be caused by heterogeneities within the natural sample as each data point was obtained from a different aliquot of the mud.

The range of particle concentrations over which a yield stress can be measured for the hemipelagic sediment is approximately between 10% and 20%. Below a concentration of 10% the particles settle creating a muddy fluid top layer and particle rich layer underneath. Comparing the results with other studies that used sediment suspensions, the hemipelagic marine sediment is able to develop a static stress at comparatively low particle concentrations (Figure 2a). Additionally, other studies that measured yield stresses at low particle concentrations were kaolinite and water mixtures produced in the lab (Figure 2a—laboratory-produced mixtures are represented with squares).

The clay content in the hemipelagic sediment is in the higher range compared to the other studies shown in Figure 2a, although not all studies record clay content. The hemipelagic sediment has approximately 31% clay, which could be one of the contributing factors to why there is a yield stress at such low particle concentrations. Huang and García (1998) measure a yield stress at lower concentration, approximately 7%, but

**Table 1***The Hemipelagic Sediment and Salton Sea Sediment Measured in This Study*

Sample	Particle concentration (%)	Dynamic yield (Pa)	Consistency (Pa·s)	Static yield (Pa)	Density (g/cm <sup>3</sup> )	% Clay	<i>n</i>
Hemipelagic marine sediment	19.4 ± 1.1%	701.9 ± 2.6	126.4 ± 5.8	1440.9 ± 1.5	1.34	31	3.5
	17.8 ± 0.8%	111.4 ± 2.8	71.1 ± 4.1	634.2 ± 17.4	1.31	31	3.5
	16.9 ± 2.5%	218.1 ± 2.1	104.8 ± 3.5	445.3 ± 13.9	1.29	31	3.5
	12.4 ± 1.1%	39.8 ± 0.2	15.5 ± 0.6	265.3 ± 3.2	1.22	31	3.5
	15.1 ± 1.1%	56.3 ± 0.7	35.5 ± 2.2	211.1 ± 9.4	1.27	31	4.5
	10.4 ± 0.9%	66.5 ± 0.3	20.0 ± 0.9	173.1 ± 5.6	1.18	31	3.5
	9.9 ± 0.9%	20.5 ± 0.6	8.9 ± 1.4	108.1 ± 7.3	1.17	31	3.6
	10.1 ± 1.2%	18.3 ± 0.5	13.1 ± 1.0	53.3 ± 3.9	1.18	31	3.5
Salton Sea mud volcano	44.2 ± 1.45%	769.1 ± 3.0	95.4 ± 22.3	1247.8 ± 2.6	1.76	26	3.5
	42.9 ± 1.6%	353.6 ± 0.7	125.1 ± 1.9	893.4 ± 0.2	1.73	26	3.5
	41.7 ± 1.6%	291.1 ± 0.8	11.4 ± 4.7	458.3 ± 0.9	1.7	26	3.5
	40.5 ± 1.6%	189.4 ± 0.9	15.5 ± 8.2	229.7 ± 11.1	1.67	26	3.5
	40.5 ± 1.8%	145.3 ± 0.5	9.3 ± 4.9	55.8 ± 20.1	1.68	26	3.5

Note. \*Dynamic yield and consistency fit with Bingham model. \*\* static yield and n fit with the Herschel-Bulkley model. Data plotted in Figure 2.

do not record the clay content of the sample they used. The higher clay content increases electrostatic forces between the clay particles. Yu et al. (2013) found that increasing the clay content from approximately 10% to 40% clay increased the yield stress by more than an order of magnitude, consistent with Jeong (2013) who reported the highest clay content and similarly large yield stresses. While both the hemipelagic sediment and Salton Sea mud have kaolinite, illite, montmorillonite, the hemipelagic sediment also contains smectite, which is highly cohesive. The addition of this clay type could also contribute to the higher yield stress and more thixotropic behavior compared to the Salton Sea mud. The yield stress of the hemipelagic sediment is also more than an order of magnitude larger than kaolinite suspensions with similar particle concentrations suggesting that the presence of smectite is largely responsible for the higher yield stress (in Figure 2, compare Huang & Garcia, 1998, and Maciel et al., 2009, data with the present measurements).

The salinity of the hemipelagic sediment, at 35 g/L, is well above the salinity that Perret et al. (1996) identify as influencing rheology. Above this salinity, there is fast reconstruction of the microstructure, and below the material is likely to favor slower reconstruction. Yang et al. (2014), however, found no effect on rheology of salinity in the range of fresh water to 50 g/l salinity. Using the method outlined by Perret et al. (1996), to determine the thixotropic nature of a material, the area between the hemipelagic sediment thixotropy test curves is larger than that of the Salton Sea sediment, indicating that the hemipelagic material is slower to recover back to its initial state. This indicates that the clay content has a larger effect than salinity for the two samples we considered.

Materials with high clay contents have a slow rate of reconstruction, increasing their recovery time (Barnes, 1997). This is also the case for the two samples we considered. While the Salton Sea mud has a significant portion of clay, the median particle size of the hemipelagic sediment is much smaller at 5.5 microns, compared to the Salton Sea sediment 35.7 microns, which could account for the difference in recovery times.

### 5.1. Particle Settling Through Seafloor Sediment

Hemipelagic sediment often contains isolated “dropstones” delivered by melting icebergs or volcanic eruptions; in the case of sediments offshore the Lesser Antilles volcanic arc, these are predominately pumice clasts, deposited from rafts of pumice or fall out. Whether these clasts are preserved within their deposit or subsequently sink multiple clast diameters through underlying layers depends on their size and weight. In order to determine whether a larger particle with radius  $R_0$  can settle within mud, we approximate the clast as a completely submerged sphere. The effective weight is

$$F = \frac{4}{3}\pi(\rho_s - \rho)R_0^3g, \quad (5)$$

where  $\rho_s$  is the density of the sphere ( $\text{kg/m}^3$ ),  $\rho$  is the density of the mud,  $R_0$  is the radius of the sphere (m), and  $g$  is gravity ( $\text{m/s}^2$ ). The density of the sediment depends on the particle concentration ( $\phi$ ),  $\rho = \rho_s\phi + \rho_w(1-\phi)$ . The sphere will cause yielding of the mud and sink when the yield stress parameter

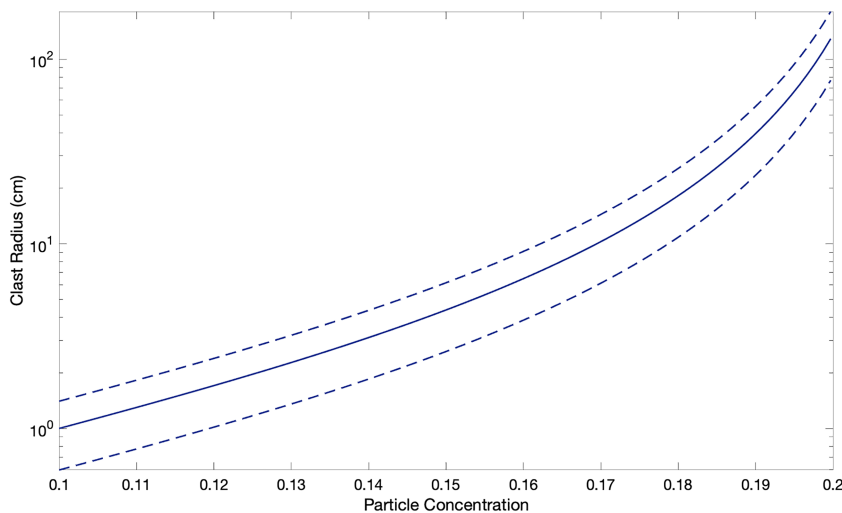


**Figure 3.** Particle concentration of hemipelagic sediment and the clast radius that would exceed the yield stress parameter defined by Beris et al. (1985). For radii above the blue curve, clasts will settle through the hemipelagic marine sediment. Clasts are approximated as spheres of density 1.65 g/cm<sup>3</sup>.

$$Y_g = \frac{2\tau_y \pi R_0^2}{F} \quad (6)$$

exceeds a critical value of 0.143 (Beris et al., 1985). Pumice is porous, between 60% and 80% porosity, and at the bottom of the seafloor these pores will be filled with water. The mean density was calculated assuming 60% porosity, a glass density of 2,700 kg/m<sup>3</sup> and a sea water density of 1030 kg/m<sup>3</sup>. We use a dynamic yield stress because we assume the clasts are initially moving when they reach the seafloor. Using equations (6) and (3) to determine the yield stress as a function of particle concentration, we calculate the relationship between the particle concentration and the radius of a clasts that would settle through the sediment (Figure 3). Below this radius, clasts would not settle but instead be preserved in situ. Using an average mud particle concentration at the seafloor of 10% (Hamilton, 1976) a pumice clast would have to have a radius larger than about 1 cm to settle through uncompacted hemipelagic sediment. Most of the various volcanic dropstones collected during IODP 340 (le Friant et al., 2013; Jutzeler et al., 2016) are thus in place and their stratigraphic locations record the time of eruptions.

## 6. Conclusion

By studying the rheology of a naturally occurring mud we can better discern some of the influencing factors in rheology and thixotropic behavior. Particle concentration affects the yield stress and consistency, with increasing particle concentrations leading to increasing yield stresses and consistency. As particle concentration increases, the thixotropic behavior also increases and the material becomes more history dependent. The particle concentration of the material also dictates the sizes of clasts that can settle through seafloor sediment. Pumice clasts would need radii greater than ~1 cm to settle through the hemipelagic sediment, indicating that most pumice clasts collected in IODP 340 are stratigraphically in place. Finally, the high smectite clay content in the hemipelagic sediment leads to more attractive colloidal forces in the sample and appears to influence the yield stress and enhance the thixotropic nature of the material.

## References

- Baas, J. H., & Best, J. L. (2002). Turbulence modulation in clay-rich sediment-laden flows and some implications for sediment deposition. *Journal of Sedimentary Research*, 72(3), 336–340. <https://doi.org/10.1306/120601720336>
- Barnes, H. A. (1997). Thixotropy—A review. *Journal of Non-Newtonian Fluid Mechanics*, 70(1-2), 1–33. [https://doi.org/10.1016/S0377-0257\(97\)00004-9](https://doi.org/10.1016/S0377-0257(97)00004-9)

## Acknowledgments

This research used samples provided by the Integrated Ocean Drilling Program (IODP). Funding for this research was provided by a Post Expedition Activity award and completed with NSF EAR 1615203. We thank ANR-13-BS06-0009, Labex UnivEarth and Interreg Caraibes PREST for funding. The dedication and hard work of entire staff and scientific party on the Joides Resolution contributed to the sampling and analyses that made the present measurements possible, in particular O. Ishizuka, and staff scientists N. Stroncik and A. Klaus. Additional support was provided from the National Science Foundation. Aaron Tran and Max Rudolph helped with the sampling and analysis of the Salton Sea muds. Laurel Larson provided the particle size analyzer. Dula Parkinson guided the XRay tomography and reconstruction, and beamtime was provided by the ALS at LBNL. Tim Teague performed the XRD measurements and analysis. Rheologic measurements are available on [https://github.com/eknappe/rheology\\_tech\\_reports](https://github.com/eknappe/rheology_tech_reports). We thank two reviewers for constructive comments and suggestions.

- Beris, A. N., Tsamopoulos, J. A., Armstrong, R. C., & Brown, R. A. (1985). Creeping motion of a sphere through a Bingham plastic. *Journal of Fluid Mechanics*, 158, 219–244. <https://doi.org/10.1017/S0022112085002622>
- Blasio, F. V., Breien, H., & Elverhøi, A. (2011). Modelling a cohesive-frictional debris flow: An experimental, theoretical and field-based study. *Earth Surface Processes and Landforms*, 36(6), 753–766. <https://doi.org/10.1002/esp.2101>
- Brunet, M., Le Friant, A., Boudon, G., Lafuerza, S., Talling, P., Hornbach, M., et al., & IODP Expedition 340 Science Party (2016). Composition, geometry, and emplacement dynamics of a large volcanic island landslide offshore Martinique: From volcano flank-collapse to seafloor sediment failure? *Geochemistry Geophysics Geosystems*, 17(3), 699–724. <https://doi.org/10.1002/2015GC006034>
- Coussot, P., Leonov, A. I., & Piau, J. M. (1992). Rheologic modeling and peculiar properties of some debris flows, *Proceedings of International Symposium on Erosion, Debris Flows and Environment in Mountain Regions*, (pp. 207–216). I.A.H.S. Publication 209, Wallingford, Oxfordshire, UK.
- Coussot, P., & Piau, J. M. (1994). On the behavior of fine mud suspensions. *Rheologica Acta*, 33(3), 175–184. <https://doi.org/10.1007/BF00437302>
- Coussot, P., Proust, S., & Ancey, C. (1996). Rheological interpretation of deposits of yield stress Fluids. *Journal of Non-Newtonian Fluid Mechanics*, 66(1), 55–70. [https://doi.org/10.1016/0377-0257\(96\)01474-7](https://doi.org/10.1016/0377-0257(96)01474-7)
- de Souza Mendes, P. R. (2009). Modeling the thixotropic behavior of structured fluids. *Journal of Non-Newtonian Fluid Mechanics*, 164(1–3), 66–75. <https://doi.org/10.1016/j.jnnfm.2009.08.005>
- Dullaert, K., & Mewis, J. (2006). A structural kinetics model for thixotropy. *Journal of Non-Newtonian Fluid Mechanics*, 139(1–2), 21–30. <https://doi.org/10.1016/j.jnnfm.2006.06.002>
- Hamilton, E. L. (1976). Variations of density and porosity with depth in deep-sea sediments. *Journal of Sedimentary Petrology*, 46, 280–300.
- Huang, X., & García, M. H. (1998). A Herschel-Bulkley model for mud flow down a slope. *Journal of Fluid Mechanics*, 374, 305–333.
- Imran, J., Parker, G., Locat, J., & Lee, H. (2001). 1D Numerical model of muddy subaqueous and subaerial debris flows. *Journal of Hydraulic Engineering*, 127(11), 959–968. [https://doi.org/10.1061/\(ASCE\)0733-9429\(2001\)127:11\(959\)](https://doi.org/10.1061/(ASCE)0733-9429(2001)127:11(959))
- Jeong, S. W. (2010). Grain size dependent rheology on the mobility of debris flows. *Geoscience Journal*, 14(4), 359–369. <https://doi.org/10.1007/s12303-010-0036-y>
- Jeong, S. W. (2013). Determining the viscosity and yield surface of marine sediments using modified Bingham models. *Geosciences Journal*, 17, 241–247.
- Jutzeler, M., Manga, M., White, J. D. L., Talling, P. J., Proussevitch, A. A., Watt, S. F. L., et al. (2016). Submarine deposits from pumice-rich pyroclastic density currents dispersing over water: An outstanding example from offshore Montserrat (IODP 340). *Bulletin of the Geological Society of America*. <https://doi.org/10.1130/B31448.1>
- Lafuerza, S., Le Friant, A., Manga, M., Boudon, G., Villemant, B., Stroncik, N., et al., & Expedition 340 Scientific Party (2014). Geomechanical characterizations of submarine volcano flank sediments, Martinique, Lesser Antilles Arc. In S. Krastel, et al. (Eds.), *Submarine mass movements and consequences, Advances in Natural and Technological Hazards Research* (pp. 73–81). Switzerland, 2014, 37: Springer Inten. Publishing. [https://doi.org/10.1007/978-3-319-00972-8\\_7](https://doi.org/10.1007/978-3-319-00972-8_7)
- Le Friant, A., Ishizuka, O., Boudon, G., Palmer, M. R., Talling, P., Villemant, B., et al. (2015). Submarine record of volcanic island construction and collapse in the Lesser Antilles arc: First scientific drilling of submarine volcanic island landslides by IODP Expedition 340. *Geochemistry, Geophysics, Geosystems*, 16(2), 420–442.
- Le Friant, A., Ishizuka, O., Stroncik, N. A., and the Expedition 340 Scientists 2013, Lesser Antilles Volcanism and Landslides, Integrated Ocean Drilling Program Expedition 340 Preliminary Report, doi:10.2204/iodp.pr.340.2012.
- Le Friant, A., Lock, E. J., Hart, M. B., Boudon, G., Sparks, R. S. J., Leng, M. J., et al. (2008). Late Pleistocene tephrochronology of marine sediments adjacent to Montserrat, Lesser Antilles volcanic arc. *Journal of the Geological Society, London, (London, U.K.)*, 165(1), 279–289. <https://doi.org/10.1144/0016-76492007-019>
- Locat, J., Lee, H. J., Locat, P., & Imran, J. (2004). Numerical analysis of the mobility of the Palos Verdes debris avalanche, California, and its implication for the generation of tsunamis. *Marine Geology*, 203, 269–280.
- Maciel, G. F., Santos, H. K., & Ferreira, F. O. (2009). Rheological analysis of water clay compositions in order to investigate mudflows developing in canals. *Journal of the Brazil Society of Mechanical Science and Engineer*, 31, 64–74.
- Mader, H. M., Llewellyn, E. W., & Mueller, S. P. (2013). The rheology of two-phase magmas: A review and analysis. *Journal of Volcanology and Geothermal Research*, 257, 135–158. <https://doi.org/10.1016/j.jvolgeores.2013.02.014>
- Malet, J. P., Laigle, D., Remaitre, A., & Maquaire, O. (2005). Triggering condition and mobility of debris flows associated to complex earthflow. *Geomorphology*, 66, 215–235.
- Manga, M., & Bonini, M. (2012). Large historical eruptions at subaerial mud volcanoes, Italy. *Natural Hazards and Earth System Science*, 12(11), 3377–3386. <https://doi.org/10.5194/nhess-12-3377-2012>
- Marr, J. G., Harff, P. A., Shanmugam, G., & Parker, G. (2001). Experiments on subaqueous sandy gravity flows: The role of clay and water content in flow dynamics and depositional structures. *GSA Bulletin*, 113(11), 1377–1386.
- Menapace, W., Tanguan, D., Maas, M., Williams, T., & Kopf, A. (2019). Rheology and biostratigraphy of the Marañon serpentine muds unravel mud volcano evolution. *Journal of Geophysical Research*, 124(11), 10752–10776. <https://doi.org/10.1029/2019JB018265>
- Moller, P., Fall, A., Chikkadi, V., Derkks, D., & Bonn, D. (2009). An attempt to categorize yield stress fluid behavior. *Philosophical Transactions of the Royal Society*, 367, 5139–5155.
- Mueller, S., Llewellyn, E. W., & Mader, H. M. (2009). The rheology of suspensions of solid particles. *Proceedings of the Royal Society*, 466, 1201–1228.
- Palmer, M., Hatter, S. J., Gernon, T. M., Taylor, R. N., Cassidy, M., Johnson, P., et al. (2016). Discovery of a large 2.4 Ma Plinian eruption of Basse-Terre, Guadeloupe, from the marine sediment record. *Geology*, 44(2), 123–126. <https://doi.org/10.1130/G37193.1>
- Perret, D., Locat, J., & Martignoni, P. (1996). Thixotropic behavior during shear of a fine-grained mud from Eastern Canada. *Engineering Geology*, 43(1), 31–44. [https://doi.org/10.1016/0013-7952\(96\)00031-2](https://doi.org/10.1016/0013-7952(96)00031-2)
- Remaitre, A., Malet, J. P., Maquaire, O., Ancey, C., & Locat, J. (2005). Flow behavior and runout modeling of a complex debris flow in a clay-shale basin. *Earth Surface Processes and Landforms*, 30(4), 479–488. <https://doi.org/10.1002/esp.1162>
- Santolo, A. S., & Evangelista, A. (2005). Some observations on the prediction of the dynamic parameters of debris flows in pyroclastic deposits in the Campania region of Italy. *Natural Hazards*, 50, 605–622.
- Santolo, A. S., Pellegrino, A. M., & Evangelista, A. (2010). Experimental study on the rheologic behavior of debris flow. *Natural Hazards Earth System Science*, 10, 2507–2514.

- Santolo, A. S., Pellegrino, A. M., Evangelista, A., & Coussot, P. (2012). Rheologic behavior of reconstituted pyroclastic debris flow. *Geotechnique*, 62, 19–27.
- Svensen, H., Hammer, O., Mazzini, A., Onderdonk, N., Polteau, S., Planke, S., & Podladchikov, Y. Y. (2009). Dynamics of hydrothermal seeps from the Salton Sea geothermal system (California, USA) constrained by temperature monitoring and time series analysis. *Journal of Geophysical Research*, 114, B09201. <https://doi.org/10.1029/2008JB006247>
- Talling, P. J. (2013). Hybrid submarine flows comprising turbidity current and cohesive debris flow: Deposits, theoretical and experimental analyses and generalized models. *Geosphere*, 9(3), 460–488. <https://doi.org/10.1130/GES00793>
- Tran, A., Rudolph, M. L., & Manga, M. (2015). Bubble mobility in mud and yield stress fluids. *Journal of Volcanology and Geothermal Research*, 294, 11–24. <https://doi.org/10.1016/j.jvolgeores.2015.02.004>
- Treger, N. A., Pakula, M. E., & Shah, S. P. (2010). Influence of clays on the rheology of cement pastes. *Cement and Concrete Research*, 40(3), 384–391. <https://doi.org/10.1016/j.cemconres.2009.11.001>
- Van Kessel, T., & Blom, C. (1998). Rheology of cohesive sediments: Comparison between anatural and an artificial mud. *Journal of Hydraulic Research*, 36(4), 591–612. <https://doi.org/10.1080/00221689809498611>
- Yang, W. Y., Yu, G.-L., Tan, S., & Wang, H. K. (2014). Rheological properties of dense natural cohesive sediments subject to shear loadings. *International Journal of Sediment Research*, 29(4), 454–470. [https://doi.org/10.1016/S1001-6279\(14\)60059-7](https://doi.org/10.1016/S1001-6279(14)60059-7)
- Yu, B., Ma, Y., & Qi, X. (2013). Experimental study on the influence of clay mineral on the yield stress of debris flows. *Journal of Hydraulic Engineering*, 139(4), 364–373. [https://doi.org/10.1061/\(ASCE\)HY.1943-7900.0000679](https://doi.org/10.1061/(ASCE)HY.1943-7900.0000679)